Cold Regions Science and Technology 114 (2015) 44–60

Contents lists available at ScienceDirect

Cold Regions Science and Technology

journal homepage: www.elsevier.com/locate/coldregions

Evaluating ablation and environmental impact of giant anthropogenic snow patches (Yuzhno-Sakhalinsk, Russia)

Evgeny A. Podolskiy [a,*], Valentina A. Lobkina [b], Yuri V. Gensiorovsky [b], Emmanuel Thibert [c,d]

[a] Institute of Low Temperature Science, Hokkaido University, Kita-19, Nishi-8, Kita-ku, Sapporo 060-0819, Japan
[b] Sakhalin Department of Far East Geological Institute, Far East Branch of Russian Academy of Sciences, 25 Gor'kogo St., 694023 Yuzhno-Sakhalinsk, Russia
[c] Irstea, UR ETGR, Centre de Grenoble, 2 rue de la Papeterie, BP 76, F-38402 St.-Martin-d'Hères, France
[d] Univ. Grenoble Alpes, F-38000 Grenoble, France

ARTICLE INFO

Article history:
Received 15 November 2014
Received in revised form 23 February 2015
Accepted 2 March 2015
Available online 7 March 2015

Keywords:
Snow patch
Snow disposal
Pollution
Urban environment
Street cleaning
Snow chemistry

ABSTRACT

Systematic snow disposal from street cleaning operations may create large anthropogenic snow/ice bodies. Such man-made cryospheric objects may be considered as complex geophysical interfaces between the atmosphere, landscape, soils and hydrosphere. Urban snow patches not only produce large amounts of meltwater (and therefore a risk of flooding), but also serve as multiphase chemical reactors due to highly polluted mixture of snow/ice with various materials and water inclusions. However, the exact roles of snow patches in the environment and the factors driving their temporal evolution remain unclear. They are nevertheless of major importance for informed decision making and sustainable disposal operations. Here we present the results of a 4-year monitoring program concerning two artificial snow patches near the town of Yuzhno-Sakhalinsk (Russia) and the results of numerical modeling inferring the main corresponding processes, i.e. melting and water discharges. The temperature-based index method proved adequate to assess the evolution of the two snow patches. Constant ablation factors of about 0.45–0.58 and 0.27–0.31 cm w.e. d^{-1} $°C^{-1}$, respectively, were found to be appropriate for a first order approximation of snow patch melt dynamics. However, twice lower melt rates were found for one of the two closely located snow patches. This suggests that other factors, such as debris content, likely play a role. This difference in melting can be accounted for by modulating the ablation factor according to debris properties. In terms of peak daily water discharge, snow patch melting produces about 5–15 cm w.e. per day, comparable to rain rates during regional typhoons. This study represents a starting point that should be followed by a more detailed monitoring program and the application of a more complex numerical model of snow disposal sites, to allow optimization of their maintenance. For example, marginal melting or the combined influence of debris and soils on surface runoff should be further investigated. Moreover, better constrained and formulated chemical processes will allow a more reliable estimate of the local environmental impact of regular snow disposal.

1. Introduction

Storage of snow removed from urban areas at particular locations may lead to environmental disasters (Gensiorovsky et al., 2013; Lobkina and Gensiorovsky, 2012). In heavy snowfall regions, like Sakhalin Island, Russia, more than a million cubic meters of snow is annually transported from city streets (e.g. Gensiorovsky, 2010) to deposit sites. This can have a significant impact on the environment. In particular, the following mechanisms have been identified (Gensiorovsky et al., 2013): i) a large anthropogenic snow-ice body can survive the ablation season and lead to the discharge of polluted meltwater localized in space and time; ii) repetitive water discharge has bio-geo-chemical impacts as it cumulatively increases concentration of pollutants in soils, killing flora and leaking further into the hydrosphere with potentially severe ecological effects on water bodies (Goto-Azuma, 1998; Tsiouris et al., 1985); iii) large amounts of meltwater can lead to flooding, the formation of swamps and gradual degradation of the surrounding ecosystem and infrastructure (e.g. erosion of roads), and iv) permafrost may be formed in areas where it does not occur naturally (Lobkina and Gensiorovsky, 2012). From this perspective, monitoring and environmental assessments of such artificial snow patches are essential for sustainable management of a territory, urban planning and associated decision and policy making. Such monitoring requires not only observations at the snow patch, but also in the urban area itself with a focus on snow accumulation and the amounts and chemical composition of the snow removed from the streets. This knowledge is crucial for

* Corresponding author.
E-mail address: evgeniy.podolskiy@gmail.com (E.A. Podolskiy).

http://dx.doi.org/10.1016/j.coldregions.2015.03.001

optimization of disposal operations and the assignment of snow disposal sites (e.g. Campbell and Langevin, 1995a,1995b).

Naturally formed snow patches are known to produce complex feedback to climate and have been relatively well studied (Fujita et al., 2010). However, artificially produced snow patches are rarely investigated, but present a challenging environmental problem, for example, in the town of Yuzhno-Sakhalinsk, with an area of 164.7 km^2 (Sakhalin, Russia). In this town, all snow is stored each year in 2 sites that have been monitored since winter 2010/2011 through several campaigns. This has produced records providing valuable material for the analysis presented herein.

Russia presently lacks special regulations to control the negative effects of snow disposal on the environment (Lobkina and Gensiorovsky, 2012). Some northern countries (e.g. Canada) have such regulations, even if mitigation measures are still lacking. This study therefore deals with an important and timely question. Furthermore, it is known that in summer, snow storage may be used to satisfy cooling demands for various facilities and processes, as described for example by Skogsberg and Nordell (2001). This potential for harvesting the cooling energy of meltwater provides additional motivation for investigating the issue of snow storage and associated pollution (Feiccabrino et al., 2008).

In this study, we attempt to construct a simple unifying framework to make it possible to use available records while overcoming the lack of certain measurements. More particularly, we want to evaluate ablation and the environmental impact of the artificial snow patches near Yuzhno-Sakhalinsk to help those in charge of making decisions concerning snow disposal strategy. To achieve these objectives, we will first present and combine all available relevant knowledge, then describe the modeling approach for melting, estimate unknown variables and associated uncertainties, reproduce the observed evolution of the snow deposit in time and finally attempt to estimate the amount of meltwater and pollutants discharged into the soil and contaminating neighboring ecosystems. The latter is important when planning snow deposits (Reinosdotter and Viklander, 2005), in particular, for the design of snowmelt drainage and water treatment systems, the necessity of which has been pointed out by Lobkina and Gensiorovsky (2012).

2. Study sites and available observations

2.1. Urban snow cleaning

About 3–5 × 10^6 m^3 of snow is annually removed from Yuzhno-Sakhalinsk streets over the winter season (between November and March) (Gensiorovsky, 2010; Gensiorovsky et al., 2013) and a portion of this snow is hauled by trucks to two disposal sites. Snow from the northern sector of the town is transported to snow patch #1 (mainly from a territory neighboring its thermal power station, Ukrainskaya street and an area of a wholesale trading base); while snow from the central and southern sectors is hauled to snow patch #2. The usual truck load volume is about 10–12 m^3 (sometimes 7 or 20 m^3) depending on the type of a vehicle. Accordingly, the annual average number of truckloads of snow is in the order of a few 10^5, which is comparable to snow disposal operations of such large cities as Montreal (Campbell and Langevin, 1995a). This highlights the challenging nature of the work and the amount of resources needed for the relatively small town of Yuzhno-Sakhalinsk (with a population of about 182,000).

Episodic evaluations of snow accumulation and removal within the urban area of Yuzhno-Sakhalinsk have been performed by Gensiorovsky (2010), Lobkina and Gensiorovsky (2012) and other studies have also looked at the snow chemistry (Gensiorovsky et al., 2013; Lobkina and Gensiorovsky, 2012). Usually the undisturbed snowpack in the urban area completely melts in April, as was the case in 2011 (Lobkina and Gensiorovsky, 2012).

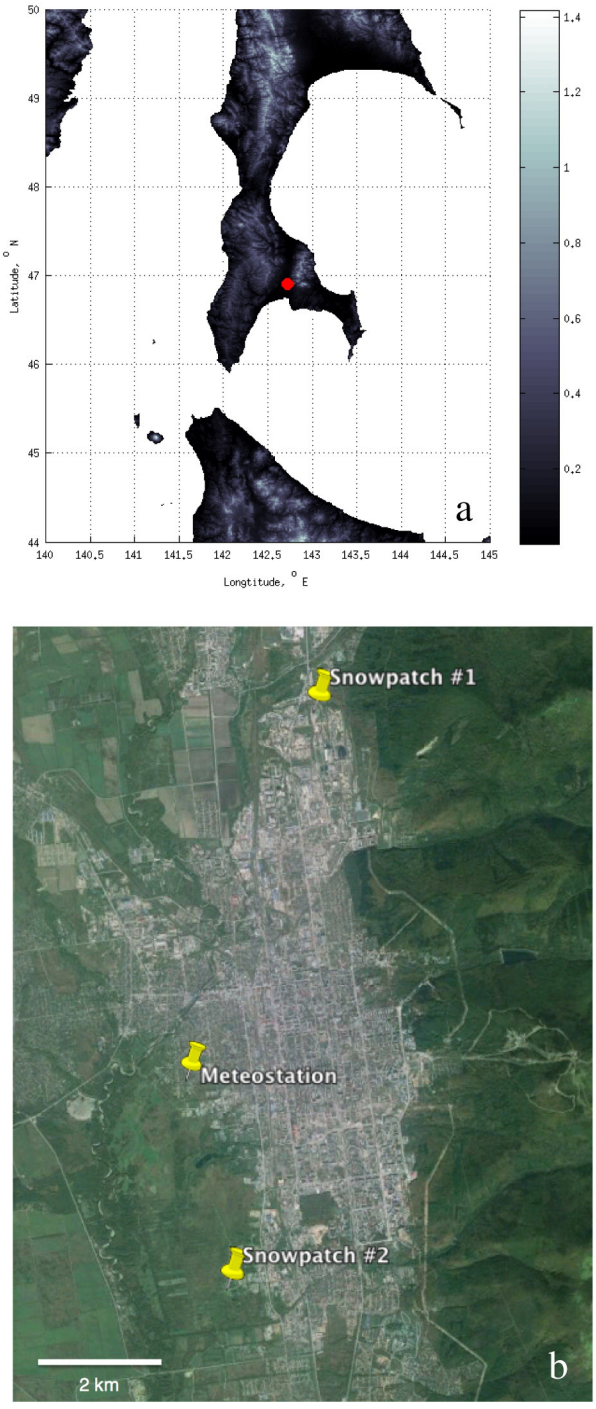

Fig. 1. a) Location of the study site (the color bar indicates the elevation in km) and b) a plan view of the town of Yuzhno-Sakhalinsk (from Google Earth) showing the exact locations of the two snow patches and the weather station. (For interpretation of the references to color in this figure legend, the reader is referred to the web version of this article.)

2.2. Snow disposal sites

The snow disposal sites have been monitored on a mostly irregular time basis by the Sakhalin Department of Far East Geological Institute since winter season 2010/2011 (Gensiorovsky et al., 2013; Lobkina and Gensiorovsky, 2012). The sites are located near Yuzhno-Sakhalinsk, in the southern part of Sakhalin Island (Fig. 1). Both sites are surrounded by plains without any marked topographic shadow (for solar radiation or wind). Photographs of these sites are provided

Fig. 2. Photographs of snow storage site #1 with the corresponding time line. The numbers indicate the months of the year (photo credits: V.A. Lobkina, Yu. V. Gensiorovsky). Note that the presence of snow or ice beneath the surface was verified *in situ* for each object.

in Figs. 2 and 3, showing temporal complexity and diversity of their surface states between 2011 and 2014. The main properties of the snow patches, including area, average height, volume and surface density, are shown in Fig. 4 for 2010/11–2013/14. The water equivalent of the deposited snow was not measured directly, but is important to estimate the amount of water discharged during the ablation season and the dilution of pollutants.

Under the climatic (monsoon) and topographic conditions of this part of Sakhalin, perennial snow patches of natural origin may exist mainly due to high accumulation from snow avalanche deposits (Gensiorovsky and Kazakov, 2006; Suchkov, 2012). The latter are known to be an important factor in river discharge at Sakhalin (Gensiorovsky et al., 2006).

The dimensions of snow patch #1 are comparable to those of a natural snow patch already studied in Japan (Fujita et al., 2010). However, the surface snow density at the time of deposition at both Yuzhno-Sakhalinsk snow patches (usually more than 500 kg m^{-3}) is significantly higher due to the artificial nature of the accumulation process (see Fig. 4).

Note that the area and volume of the snow patches (Fig. 4) change with time due to several processes, including artificial deposition, natural densification and snowmelt, as well as the redistribution of deposited snow by tractors during the accumulation period. Such technical post-processing is known to increase the temperature of snow towards the melting point (J.M. Glénat, personal communication, 2013) and induce granulation (see Fig. 3 for February 2011) and densification of the snowpack. Furthermore, snow is hauled to the sites more frequently after snowfalls (during such periods densification may be slower). Even without any recent snowfalls, snow input is continuous throughout the winter season due to ongoing street cleaning.

Ever since a number of vehicles delivering or flattening snow deposits became stuck in snow patch #2 (February 2011), large heights (i.e. exceeding 20 m) have been avoided. Moreover, reduced height

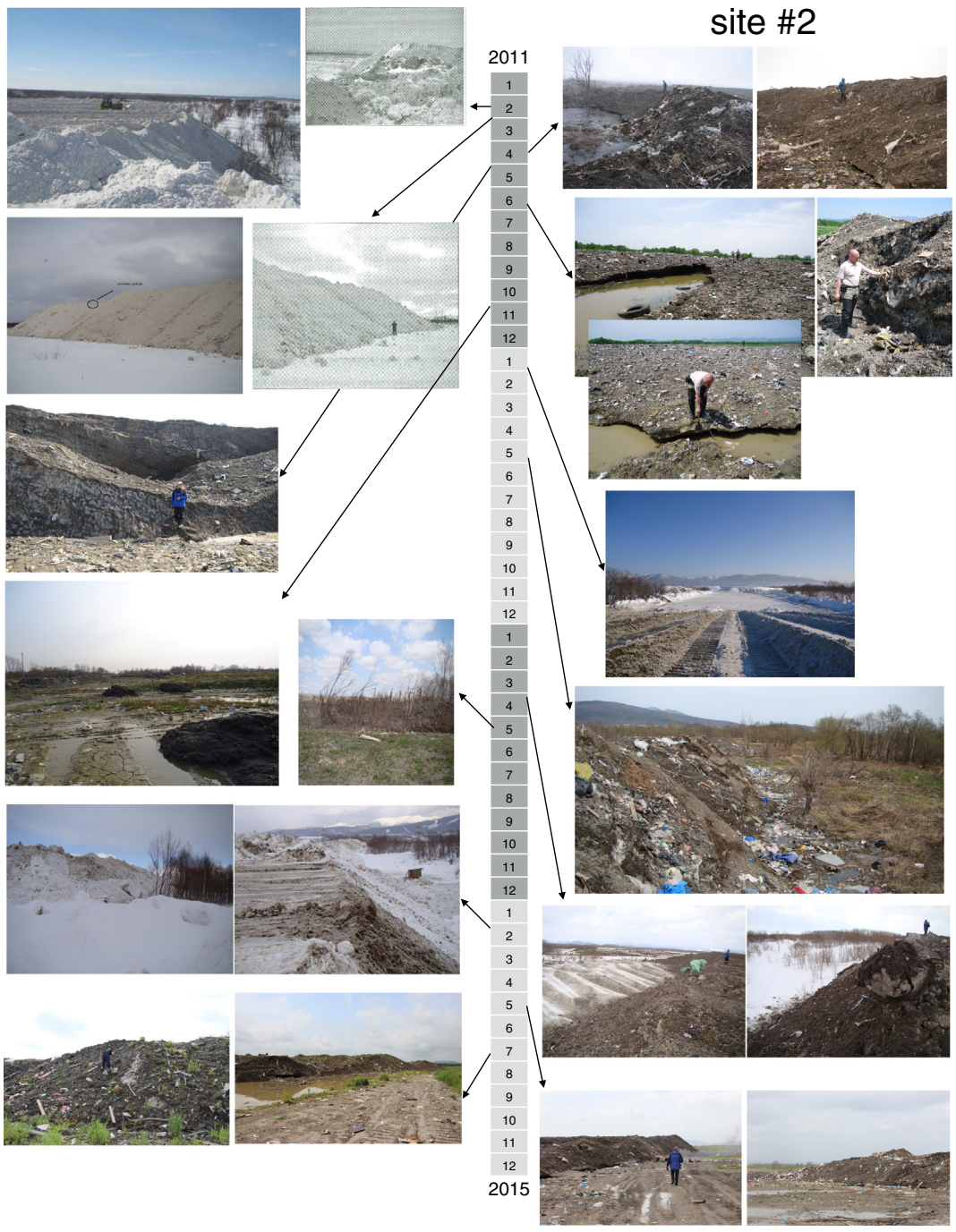

Fig. 3. Photographs of snow storage site #2 with the corresponding time line (photo credits: V.A. Lobkina, Yu. V. Gensiorovsky; black and white illustrations have been reproduced from Lobkina and Gensiorovsky (2012)). The photographs taken in November 2011 and May 2013 show the site conditions after melting and degraded plants nearby, respectively. The photograph taken in January 2012 shows the empty site before the start of main disposal operations.

and the resulting lower total water equivalent per unit area lead to faster melting, as the corresponding increase in the surface area of the snow/ice bodies enhances the energy exchange with the atmosphere.

During the ablation season, meltwater produces swamps, ponds and active streams around both snow storage sites. Large amounts of garbage (i.e. plastic, tires, wood, bottles and organic materials) and solid particle deposits are also observed. This makes field observations physically challenging due to a very unpleasant smell. Debris cover is formed by the melting-out of fine-grained lithogenic, organic and waste materials. The thickness of the debris has a high spatial variability that is difficult to quantify, especially towards the end of each melting season. Debris cover (mainly sand and clay loam) first observed in May and can subsequently increase to about 20 cm (or more in some places) by July. Grass may even start to grow on the debris cover around June (Figs. 2 and 3). The variation of surface albedo due to debris and the thermal conductivity, specific heat and density of this surface layer remain unknown.

2.2.1. Snow patch #1

Snow patch #1 is located within the northern area of the town near Prospect Mira street (47.005°N, 142.738°E, 41 masl). It is a flat area, surrounded by several industrial warehouses, which may be exposed to flooding during intensive periods of snowmelt (drainage ditch has recently been dug for this reason). In contrast to snow patch #2, this

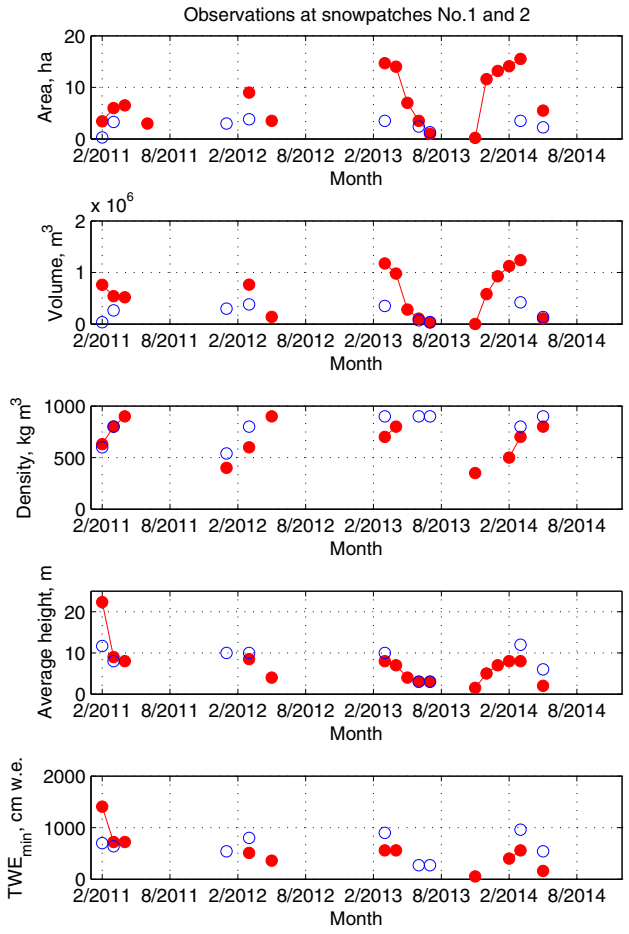

Fig. 4. Properties of snow patches #1 (blue circles) and #2 (red circles). In order to increase the number of reference points, 4 missing density values (for 5/2012, 6–7/2013 and 5/2014) were assumed to be equal to 900 kg m^{-3} based on previous measurements. (For interpretation of the references to color in this figure legend, the reader is referred to the web version of this article.)

site has a bounded area, limiting the maximum spatial extent of snow disposal to less than 4.0 ha.

In addition to the planned snow deposits, it appears to us that a lot of solid waste is disposed illegally at the site in winter. During melting periods cones of granular construction materials (up to 2–2.5 m high) were noticed at some places. This does not appear to be the case at snow patch #2, which has well organized official check-in gates for all incoming trucks.

During the last 4 ablation seasons (2011–2014), snow patch #1 did not melt completely leaving some snow for the following season. The spatial variability of height changes due to melting/settling may be significant (about 8 m), indicating relatively heterogeneous melting/settling rates. Short-term snow temperature measurements (end of July 2014) at a depth of 0.5 m showed a constant temperature of −0.4 °C over 3 days.

At the end of September 2014 the owner of the land under snow patch #1 changed. This resulted in snow patch breakage, flattening and coverage with loam. In the beginning of October 2014, the site was still surrounded by a swamp. Therefore, snow will have to be deposited elsewhere over the next winter season.

2.2.2. Snow patch #2

Snow patch #2 (Fig. 3) is located on the south-west side of Yuzhno-Sakhalinsk near Zheleznodorojnaya street (46.919°N, 142.720°E, 16 masl). This land was previously used for farming and a drainage system still in place allows meltwater to flow into the nearby Susuya River. This river however flows into Salmon Bay (Bukhta Lososey) and can produce floods (Fig. 1).

The snow thickness during the melting period varies less spatially than at snow patch #1 (about 5 m). Its surface is therefore flatter and more homogeneous (Fig. 3), making somewhat simpler to model this snow patch than snow patch #1.

According to Lobkina and Gensiorovsky (2012), this snow patch completely melted by the beginning of September 2011. The snow patch melted in July in 2012 and in August in 2013. Only in 2014 did snow patch #2 not melt completely leaving a partial deposit with an average thickness of 2 m (according to a survey on 9 October 2014). Hereafter we consider these time marks as references for model calibration.

2.3. Underlying soils

Soil properties at snow storage sites determine the amount of snowmelt (and pollutants) contributing to infiltration and surface runoff. However, due to difficult access, these properties (such as hydraulic conductivity, which determines infiltration capacity) are not accurately known. Based on a few pits, disposal site #1 seems to have a subsurface horizon of clay, separating the snow patch from the ground water.

Disposal site #2 has deposits resulting from snowmelt (gravel and sand about 10 cm thick) on top, covering a thin layer of degraded soil-vegetation and further down some clay mixed with gravel or gravel-sand with clay loam (10–30 cm). Groundwater level is only 0–15 cm below the surface. This indicates that the meltwater is in direct contact with the aquifer and that the soils are close to a saturated state.

Permafrost does not naturally develop under the climatic conditions of this part of Sakhalin Island (Gensiorovsky et al., 2013). If soil freezes before the deposition of snow, newly formed permafrost may block infiltration of meltwater into soil and therefore increase surface runoff (Feiccabrino et al., 2008). It is not clear if this situation takes place at the site of snow patch #2, where a 1 m deep swamp was observed around the deposits (May 2014). At snow disposal site #1, the freezing of upper soil layers is more likely since this snow patch survived four consequent ablation seasons, possibly insulating against the penetration of summer heat while storing cold beneath the snow. This however remains to be confirmed because meltwater generally provides latent heat when refreezing within deeper cold layers.

3. Methods (model and input data)

Below we will describe our modeling approach for estimating temporal melting of the snow patches on the basis of available observations. To evaluate melting, we employ the positive degree day (PDD) temperature model, a common and popular approach for glaciologic mass-balance modeling (e.g. Maisincho et al., 2014; Thibert et al., 2013).

We chose the temperature-based melt-index method for calibration against available data because the alternative energy balance model (e.g. Fujita et al., 2010) requires measurements of the energy fluxes at the surface layer and assumptions concerning a larger number of unknown parameters. Given that we are dealing with an optimization problem, the energy balance model would only increase the number of degrees-of-freedom in the system and therefore a number of possible solutions.

3.1. Mass-balance model

Snow density change with depth may be estimated using the following relationship (Paterson, 1994):

$$\rho(z) = \rho_i - (\rho_i - \rho_s)e^{-Cz}, \quad (1)$$

where ρ_i is the density of ice (917 kg m^{-3}), ρ_s is the surface density, $C = \frac{1.9}{z_t}$ and z_t is a depth of firn-to-ice transition.

Consequently, the total mass of a snow-ice body, M_{tot}, may be estimated as

$$M_{tot} = \int_{\Omega}\int_{-h}^{0} \rho(z) dz dA, \tag{2}$$

where Ω is an area of a snow patch and h is the thickness of the snow. Note that the inner integral

$$\int_{-h}^{0} \rho(z) dz = \rho_i \; h - (\rho_i - \rho_s)(1/C)\left(e^{Ch} - 1\right), \tag{3}$$

gives a total mass per m^2 and if divided by 10 kg (i.e. the mass of a 1 cm w.e. column per m^2) corresponds to a total water equivalent of a snow column (hereafter TWE).

The PDD model is based on a linear relationship between the sum of positive daily temperatures, PDD, and the amount of melting, A_b (in cm w.e.), expressed as

$$\mathrm{PDD} = \sum_{i=1}^{n} \frac{1}{2}(\Theta + |\Theta|), \tag{4}$$

where Θ is a mean daily air temperature and

$$A_b = \mathrm{PDD} \times \alpha \tag{5}$$

where α is a PDD factor, which lies in a range [0.27–1.16] cm w.e. d^{-1} °C^{-1} for snow and ice according to Hock (2003). Representative values of the day-degree factor are 0.48 and 0.68 cm w.e. d^{-1} °C^{-1} for snow and ice respectively. Correlation between ablation and the positive degree-day sum is interpreted in terms of turbulent heat fluxes or long-wave atmospheric radiation that correlates well with air temperature (see Fujita et al. (2010) and references within for more details). Furthermore, solar radiation is known to correlate closely with temperature (Sicart et al., 2008).

The overall mass balance equation of a snow patch may be expressed as:

$$\mathrm{TWE}(t) = A_A(t) + S_P(t) - A_b(t) - A_G(t), \tag{6}$$

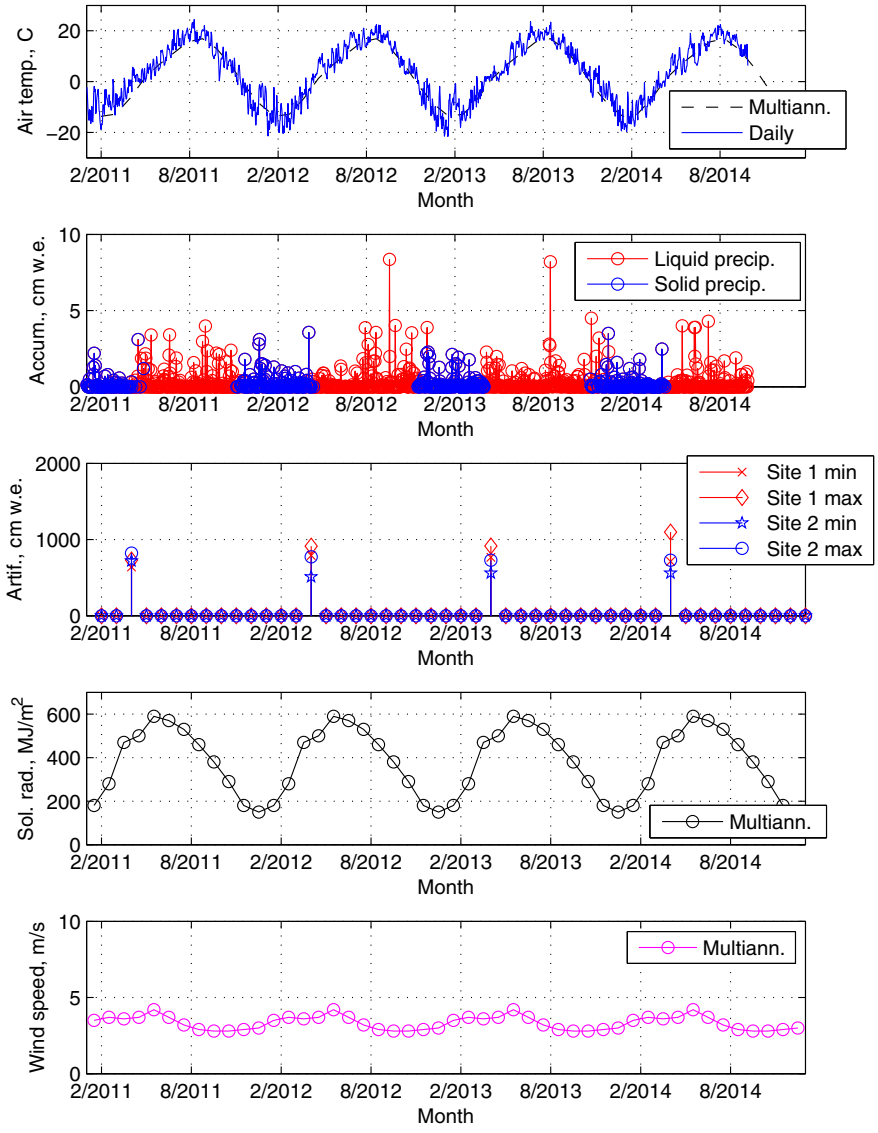

Fig. 5. Input data: meteorological time series (actual and multi-annual monthly mean values for Yuzhno-Sakhalinsk) and artificial accumulation of snow (i.e. TWE for the end of accumulation season; see text for details).

where t is the elapsed time in days, A_A is the artificial accumulation due to snow deposition by trucks, S_P the solid precipitation and A_G the melting due to geothermal flux, which is equivalent to about 1 cm w.e. per year and therefore negligible.

Solving Eq. (6) for daily time steps gives us sufficient insight into the temporal evolution of the snow patches considered in this study. For air temperature and solid precipitation (from January 2011 to September 2014), we use the mean daily values measured at the official meteorological observatory of Yuzhno-Sakhalinsk (46.950°N, 142.710°E, 22 masl), located 4 km from snow patch #2 and 6 km from snow patch #1 (Figs. 5, 6). Artificial snow accumulation, A_A (or snow disposal), is also indicated in Fig. 5 (evaluation and uncertainty of this value is discussed in details below). Note that the artificial accumulation is simply added as a 'Dirac' at the end of each accumulation season before the beginning of ablation.

We also include multiannual monthly means for the air temperature, the total amount of solar radiation and the wind speed from the same weather station (Fig. 5). Periodic extrapolation of annual air temperature time-series makes it possible to evaluate future changes and the evolution of the snow patches. Note that the winter season contribution of solid precipitation, $S_P(t)$, is negligible compared to artificial accumulation (Fig. 6).

The proposed 1D model ignores melting due to solar radiation, refreezing of meltwater within the snow patch and melting at snow patch margins. Note also that the accuracy of any temperature-based melt-index based study may be subject to year-by-year changes of the degree-day factor (Fujita et al., 2010). In order to reveal such temporal fluctuations and thereby improve the accuracy of our understanding and predictions, long-term observations are needed (but were not available in this study). In our case, however, it will be shown that α fluctuations are most likely related to debris cover changes.

3.2. Influence of debris cover

3.2.1. General features

The debris cover is made up of pollution and large amounts of litter and suspended solids (e.g. sand and dust). Snow patch albedo decreases rapidly with time as the surface debris thickness increases.

It is known that albedo of dirty snow along roads may be as low as 0.1 (Skogsberg, 2005), thus increasing melting due to increased absorption of solar radiation. Similarly, melting first increases on debris covered glaciers (Bozhinskiy et al., 1986). However, when the debris layer exceeds a so called 'critical thickness' (h_c) of a few cm, the opposite effect may occur, i.e. decreased or even almost no ablation due to insulation (Kayastha et al., 2000; Konovalov, 2000). For example, 10 cm and 40 cm of debris may reduce ablation by 35–66% and 59–85%, respectively (see a review by Skogsberg, 2005). This also depends on the thermal conductivity of the debris material. In Sweden, this property was employed in order to artificially insulate (with wood chips) a snow patch used for cooling purposes (Skogsberg, 2005).

In our case, the beginning of the ablation season may be intensified by the formation of a thin layer of debris until the thickness exceeds h_c, after which melting decreases. This can lead to higher ablation efficiency early in the season, which can however be counterbalanced by cooler temperatures than those observed later in the season.

In order to test such assumptions, we could employ an approach quantifying debris influence through a modified PDD factor (Juen et al., 2014; Lambrecht et al., 2011; Mayer et al., 2011). For this, instead of using the previously introduced constant α, we define a PDD factor as a function of debris thickness, i.e. $\alpha = f(h(t))$, where $h(t)$ is the thickness of the debris cover. The latter is known to increase from 0 cm in March to about 20 cm in July at both sites.

3.2.2. Debris thickness and PDD

As stated above, the complex influence of debris cover (Reznichenko et al., 2010) may be taken into account by adjusting the PDD factor as a function of h (Kayastha et al., 2000; Lambrecht et al., 2011). To the best of our knowledge, even for many detailed case studies on debris-covered glaciers, the precise shape of this curve is never obvious. In particular, the presumed increase of α at low h (i.e. $< h_c$) up to some maximum value α_m is rarely clearly demonstrated by precise measurements (Juen et al., 2014; Lambrecht et al., 2011; Mayer et al., 2011), with rare exceptions such as the debris rearrangement experiments by Kayastha et al. (2000). Therefore, most authors had no other choice than to assume some empirical or manually derived function (Juen et al., 2014; Konovalov, 2000; Lambrecht et al., 2011; Mayer et al., 2011).

According to Kayastha et al. (2000), the degree-day factor can be predicted from the thermal conductivity of a debris layer, which is, however, not available in this study. As an alternative, we could adopt the empirical shape proposed by Konovalov (2000), who, to the best of our knowledge, presents the only relative ablation rates available as a function of debris thickness over snow. Unfortunately, his work does not indicate any absolute values for the melting factor.

If we attempt to parameterize the previously published dependencies between α and h as a continuous function, the following formulation, partly adapted from Juen et al. (2014), may be proposed:

$$\alpha(h) = \begin{cases} ah^2 + bh + c & \text{if } h \le h_c, \\ ph^s & \text{if } h > h_c \end{cases} \tag{7}$$

where

$$\begin{aligned} a &= \frac{4(\alpha_0 - \alpha_m)}{h_c^2}, \\ b &= \frac{-4(\alpha_0 - \alpha_m)}{h_c}, \\ c &= \alpha_0, \\ p &= \frac{\alpha_0}{h_c^s}. \end{aligned} \tag{8}$$

Looking closely at previous studies, it may be concluded that usually $\frac{\alpha_0}{\alpha_m} \in [0.75, 0.95]$, which corresponds to a 5–25% increase in ablation; $h_c \in [1, 12]$ cm according to Reznichenko et al. (2010) and the decay exponent $s \in [-0.6354, -0.5354]$ according to data assimilated by Juen et al. (2014) and Lambrecht et al. (2011). For example, with $\alpha_0 \in [0.29, 0.67]$ cm w.e. d^{-1} °C^{-1}, the presented parameter space has an infinite number of possible solutions. The corresponding solution domain is shown in Fig. 7. To be able to solve the problem, we have to narrow down the possibilities of the parameter space. Therefore, as an optimal set, initially we adopt $\frac{\alpha_0}{\alpha_m} = 0.85$, $h_c = 5$ cm, and $s = -0.6354$ (see Section 4.2 for sensitivity tests).

Detailed knowledge of the evolution of debris thickness of snow patches with time is not available. Only episodic estimates can be

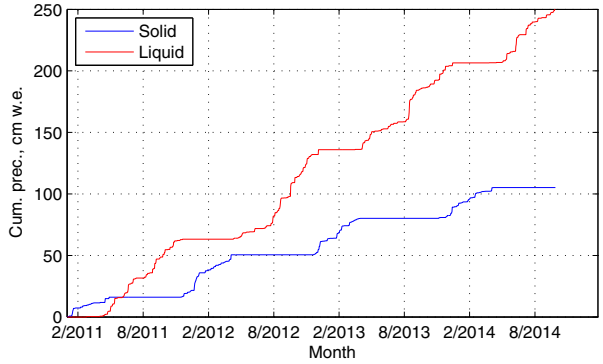

Fig. 6. Cumulative amounts of solid and liquid precipitation for 2011–2014.

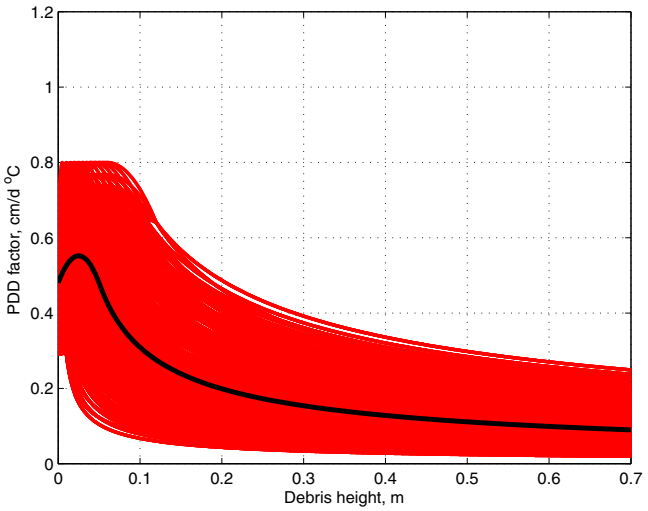

Fig. 7. Solution domain for the relationship $\alpha = f(h, h_c, \alpha_0, \alpha_m, s)$; black line shows the solution for the following parameters: $\alpha_0 = 0.48$ cm w.e. d^{-1} °C^{-1}, $\frac{\alpha_0}{\alpha_m} = 0.85$, $h_c = 5$ cm, and $s = -0.6354$.

inferred from available time referenced photographs (Figs. 2 and 3), which are provided in Fig. 8. In attempt to avoid the subjective bias of such procedure, the thickness was estimated independently by three of the co-authors as a blind test. The obtained results tend to show that the thickness exceeds a small value relatively early in the season, meaning that a possible increase of melting can only occur before this time, which corresponds to the period of the lowest temperatures of the warm season.

Temporal seasonal changes of debris thickness can be approximated (in a minimal Root Mean Square Error sense) as:

$$h(t) = 0.5 \times \left(1 + erf\left[\frac{t-\mu}{\sigma\sqrt{2}}\right]\right) \times h_{\max}, \quad (9)$$

where μ is the day of the year when the average thickness is reached (end of April), and σ is a slope (25). Assuming such a shape for every year (and setting it to 0 cm for the beginning of each winter season due to a new fallen snow cover of any surface features), we can evaluate the possible effect of debris. The presented formulation is in line with observations (Fig. 8), but is simplified because debris melt-out is a nonsteady process. Incorporation of more sophisticated feedback mechanisms with melting (e.g. Bozhinskiy et al., 1986) will require

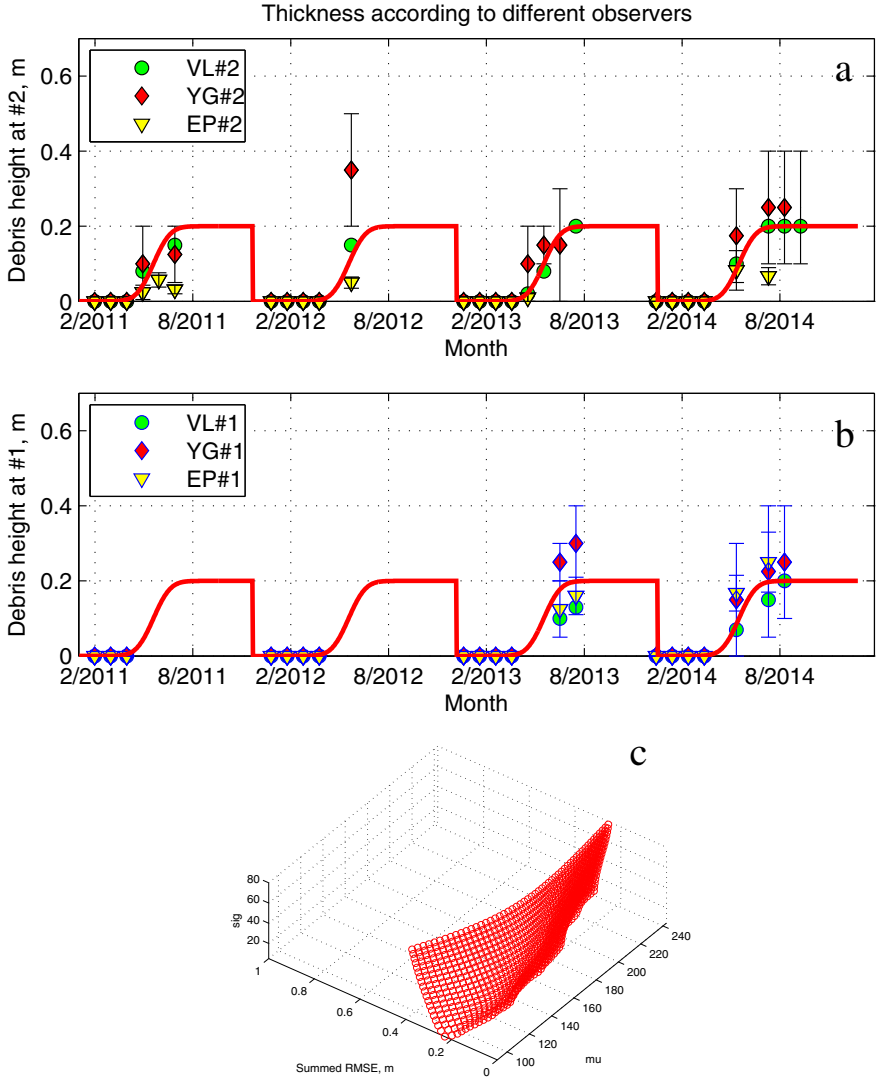

Fig. 8. a, b) Debris height, h, as a function of time according to different observers with presumed approximation curve (Eq. (9)); c) summed RMSE in response to a parameter space of the fit with its global minimum around $h_{\max} = 0.2$ m, $\mu = 140$, and $\sigma = 25$.

assumptions concerning the albedo and debris content within the body of a snow patch.

3.3. Initial conditions and constraints

Some studies of snow patches presume constant snow density over the full snowpack depth (Feiccabrino et al., 2008). This is a simplification because density actually increases with depth due to overburden pressure. In our case, the initial density profile is unknown but crucial for predicting melting over time. To address uncertainty and narrow down the possible range of TWE($\rho(z)$), we could set minimal and maximal values of the initial TWE. This could be done by fixing known parameters (h, ρ_s) and assuming unknown parameters (z_t).

For example, we could derive the $TWE_{Mar2011}$ and density profiles from two previously reported observations:

1) TWE_{min}: from the March 2011 estimates of volume of snow at the site, V, area of the snow patch, Ω, and density of snow, ρ_s, i.e.

$$A_A = \frac{V \times \rho_s}{\Omega \times 10} \tag{10}$$

which yields 720 cm w.e.

2) TWE_{max}: or, alternatively, by plugging $h = 9$ m and $\rho_s = 800$ kg m^{-3} into integrated Eq. (1) and assuming some z_t.

The relationship between TWE and z_t is illustrated in Fig. 9, which also indicates the upper limit of TWE (about 822 cm w.e.) at a very high z_t (−0.5 m). For a natural snow-ice body such a high (i.e. shallow) z_t would be unrealistic, but can be reasonable in our case due to artificial compaction of the snow patches.

On one hand, the obtained values seem to be contradictory (Fig. 10), but on the other hand, they may be considered to be a range of uncertainty, providing upper and lower limits for initial conditions (Fig. 5). Note that this advantage is a rare case in glaciology, since usually it is difficult to know the initial water equivalent of a given ice-body, for instance a glacier.

In addition, from a perspective of *in situ* observations, the introduced ambiguity highlights the importance of density profile measurements at the snow patches for reducing propagation of uncertainty through the system.

3.4. Pollution module

In an attempt to estimate the temporal evolution and amount of discharge of pollutants into the neighboring environment with meltwater,

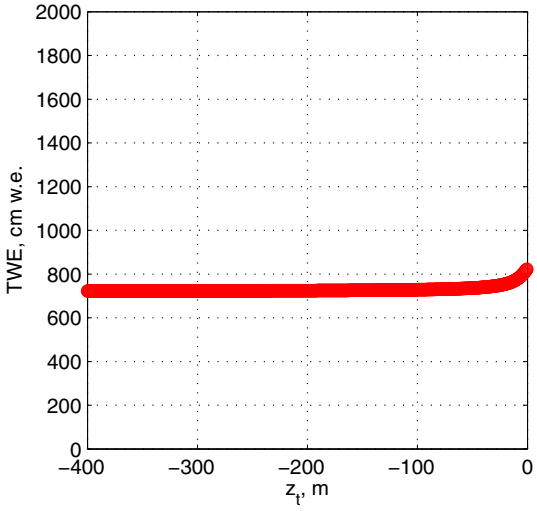

Fig. 9. Sensitivity of TWE to z_t.

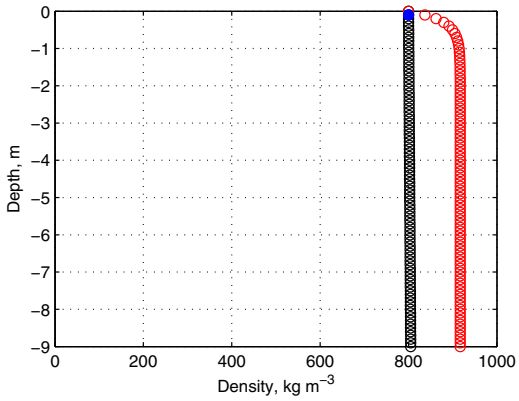

Fig. 10. Example of uncertainty in the initial density profile (black color: $z_t \to -\infty$ m; red: $z_t = -0.5$ m; blue dot indicates the measured ρ_s). Corresponding difference $\Delta TWE = 102$ cm w.e. (For interpretation of the references to color in this figure legend, the reader is referred to the web version of this article.)

we use the detailed measurements of snow chemistry at snow deposit #2 by Lobkina and Gensiorovsky (2012). Most of the chemical compounds are known to be poorly soluble in ice (Brill, 1957; Gross, 1967) and are generally located at grain boundaries in snow in highly concentrated water films and liquid inclusions (Craigin et al., 1993; Dominé and Thibert, 1995; Goto-Azuma, 1998; Wolff et al., 1989). Lobkina and Gensiorovsky (2012) measured concentrations of various molecules dissolved in the melted snow samples taken before melting season (1 March 2011), which we provide in Table 1. Note that according to Feiccabrino et al. (2008) "such samples are … very difficult to take, and do not appear to be available from any study". Due to a lack of data, Feiccabrino et al. (2008) and Lundberg et al. (2014) used snow chemistry records from other studies on snow near roads to evaluate total pollutant load in particular snow deposits at different locations. This demonstrates the unique nature of the available records.

Table 1
Chemical composition (i.e. concentrations in mg l^{-1}) of snow from different sampling sites: in the urban area, at the moment of disposal at snow patch #2, and at the edge of snow patch #2 (from Lobkina and Gensiorovsky, 2012). '–' indicates that the molecule was not found. (Cd, Cu and Pb had concentrations less than 0.01 mg l^{-1}; P and N were not found). Samples that exceed the maximum permissible concentration for fishery waters, β_{pi}, are indicated in bold.

Molecule	Urban, β_{ui}	Disposal, β_{di}	Edge, β_{ei}	Max. perm. conc., β_{pi}	$\beta_{xi} \geq \beta_{pi}$
Cations					
Li^+	–	–	0.003	0.08	
Na^+	0.56	1.17	91.7	120	
NH_4^+	0.27	**0.48**	–	0.4	Yes
K^+	0.53	0.81	1.7	50	
Ca^{2+}	0.13	0.83	23.8	180	
Mg^{2+}	0.05	0.19	1.1	40	
Anions					
F^-	–	0.02	0.14	0.75	
Cl^-	0.83	2.27	143	300	
NO_2^-	0.02	0.51	0.3	9.1	
Br^-	0.22	1.78	8.63	100	
Elements					
Al	0.01	<0.01	**0.49**	0.04	Yes
Ba	0.01	<0.01	0.04	0.74	
Ca	0.27	1.24	20.07	180	
Fe	0.01	0.02	**0.82**	0.1	Yes
K	0.25	0.09	1.93	50	
Mg	0.17	0.11	1.51	40	
Mn	<0.01	0.01	**0.05**	0.01	Yes
Na	1.08	0.55	101.0	120	
Sr	<0.01	<0.01	0.07	0.4	
Zn	**0.01**	**0.01**	**0.01**	0.01	Yes

Unfortunately, none of the analyses made for the Sakhalin snow patches considered insoluble suspended solids (e.g. road anti-skid material) in the chemical analysis of snow samples (Lobkina and Gensiorovsky, 2012). Such measurements may be of interest in the follow-up campaigns because particulate matter may carry the most significant amount of bonded pollutants (Feiccabrino et al., 2008). It also means that our estimates may be considered as a lower limit, which is likely to underestimate the total amount of pollutants. Measured amounts of total dissolved compounds in melted snow samples from the edges of sites #1 and #2 were 37 and 15 mg l^{-1}, respectively (July 2014). Furthermore, it was noted visually that meltwater from snow patch #1 seemed to be more turbid. This suggests that our evaluation based on measurements at site #2 may underestimate the amount of pollution from snow patch #1 by at least a factor of 2. Recently (May 2013), the soil chemistry at the site of snow patch #2 was documented by Gensiorovsky et al. (2013), based on samples of the soil near and under the snow patch and solid debris on the snow.

The measured pH values of meltwater discharged from snow patches #1 and #2 were mildly acidic (6.5 and 5.7, respectively; July 2013). The pH values of snow samples taken from 0.2 to 0.4 m under the snow surface were 5 and 4, respectively (July 2014). According to some reports in the literature (e.g. Feiccabrino et al., 2008), urban snow is usually more alkaline than natural snow due to suspended solids, with reported pH values for snow near roads between approximately 7.3 ± 0.38 and 8.3 ± 0.36. The corresponding concentration of suspended solids in snow melt varied between 4471 ± 3144 and 7889 ± 6744 mg l^{-1} (Feiccabrino et al., 2008).

The simplest way to evaluate the transport of elements out of the snow patch is to assume that the amount of pollutants removed directly is proportional to a unit of water equivalent, i.e.

$$P_i(t) = A_b(t) \times \beta_{di} \times 10 \tag{11}$$

where $P_i(t)$ is the outgoing mass of a particular element i (mg), and β_{di} is the concentration of the element i at the time of snow deposition (mg l^{-1}); see Table 1.

Similarly, the total pollutant load (kg) of the snow patch is

$$\mathrm{TPL}_i = \mathrm{TWE} \times \Omega \times \beta_{di} \times 10^{-5}. \tag{12}$$

This is of course a highly simplified approach to address the problem, because snow chemistry during melting is a complex process (Tsiouris et al., 1985), involving a variety of mechanisms including different responses of elements to water (Brimbelcombe et al., 1987; Cadle et al., 1984; Goto-Azuma, 1998) and photochemistry (Dominé et al., 2008). The preferential retention and release of components (elution process) from melting snow is therefore not taken into account. Nevertheless, as a first order approximation, we assume here that whatever the delay in the transport of a given element, the total amount contained in the snow patch is transferred into the soil because melting is complete (or almost complete) by the end of an ablation (Feiccabrino et al., 2008). Clearly this logic may not work for snow patch #1, which survives the ablation season. Further studies may determine whether the remaining snowpack at the end of the season can be considered to be a temporary 'accumulator' of pollutants.

4. Results and discussion

4.1. Ablation with constant α

For the period of observations, the annual average positive degree-day sum, PDD, was around 2450 ± 67 °C days. Assuming the degree-day factor = 0.48 cm w.e. d^{-1} $°C^{-1}$ (a value typical for snow (Hock, 2003)), the seasonal snow pack disappears around April (Fig. 11) as is usually observed (Lobkina and Gensiorovsky, 2012).

For the snow patches, we will first describe the results of numerical experiments with constant PDD factors, derived through calibration, and then compare them to tests made with α defined as a function of h. The two types of simulations will be plotted on the same graphs for easier comparison. The exact values of the main calibrated model parameters are summarized in Table 2.

4.1.1. Snow patch #2

The optimal factor values for snow patch #2 were found using a minimization procedure. The corresponding cost function was defined as the square root of the sum of the squared time delays from the three reference intervals of complete melting (as indicated earlier above). Indeed, the same approach could be used to fit each individual season, however we are more interested in deriving one value explaining the whole period of observations. For snow patch scenario 1 ($\mathrm{TWE}_{\min}$), the corresponding $\alpha_{\min\,2}$ is 0.45 cm w.e. d^{-1} $°C^{-1}$ and for scenario 2 ($\mathrm{TWE}_{\max}$), $\alpha_{\max\,2}$ is 0.58 cm w.e. d^{-1} $°C^{-1}$ (equivalent to peak melt rates in August of around 10–14 cm w.e. per day).

Such a range of degree-day factors is typical or slightly higher than values usually reported for snow (Hock, 2003). Given that the snow patch is composed of polluted matter and gets darker towards the end of the melting season, the obtained high value makes sense. For example, a much higher PDD factor (0.98 cm w.e. d^{-1} $°C^{-1}$) was recently reported for dirty ice by Maisincho et al. (2014).

Melting versus time for snow patch #2 and the evolution of its mass balance are shown in Fig. 11. As expected, initial TWE and PDD factor play the most important roles in the behavior of the system, namely in daily ablation intensity and dates of complete melting. In general, later melt out is caused by a higher TWE (i.e. high depth and density) or a lower value of PDD factor.

The most noticeable inconsistency between modeled and observed mass-balance for all scenarios appears in May 2014, when the observation-derived TWE is smaller than the predicted value (Fig. 11). If our TWE estimate is not wrong (due to underestimated height), this may mean that non-constant melt rates throughout the season should be considered (see also the discussion for snow patch #1 below). Another deviation from the observations is the full melt out by September 2014. This is likely the consequence of some other factors not considered in our approach. In particular, during the accumulation season of 2014 snow patch #2 had the largest area and volume for the period of observations and some self-regulation mechanisms could possibly play a role in preserving the cold state (i.e. the snow patch took a longer time to warm before melting in this specific year).

Winter season accumulation and its variability have a negligible effect on the mass-balance of the snow patch. This is not surprising given that there is more than an order of magnitude difference between annual solid precipitation (around 30 cm w.e.) and the artificial accumulation of snow. Furthermore, we could not find any relationship between the total amount of snow delivered to the snow patches and corresponding winter precipitation in 2011–2014.

We also note that the official requirement of the local authorities to close operation of snow patch #2 by the end of May (meaning that no snow should remain at the site) would appear to be physically impossible. This is illustrated in Fig. 12, which provides positive degree day sums for the last 4 years until the end of May. The average cumulative sum of positive temperatures is about 278 ± 54 °C days. For such climatic conditions, if we assume the most intense melting (α = 1.16 cm w.e. d^{-1} $°C^{-1}$) and snow density of around 800 kg m^{-3}, the height of the snow patch should be less than 4 m at the beginning of ablation season for complete melting before the end of May. With more conservative and realistic assumptions (α = 0.48 cm w.e. d^{-1} $°C^{-1}$, ρ = 600 kg m^{-3}) the height should be less than 2 m for complete melting. Flattening of the snow patch to such small heights would mean a significant increase in its area and therefore additional working hours.

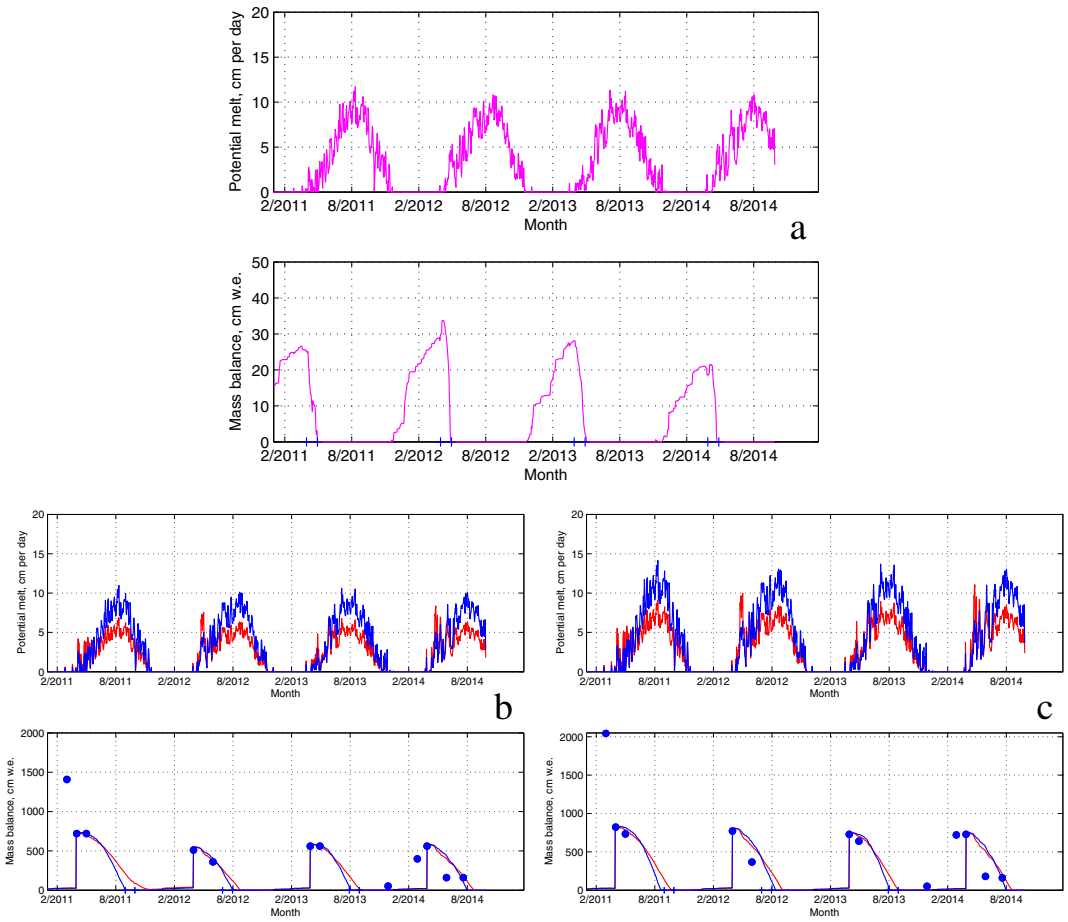

Fig. 11. Potential melting and cumulative mass-balance for 2011–2014. a) Seasonal urban snowpack, $\alpha_s = 0.48$ cm w.e. $d^{-1}\,°C^{-1}$ (intervals between the blue bars on the time axis indicate April when urban snow usually disappears); snow patch #2: b) scenario 1 (TWE_{min}), $\alpha_{min\ 2} = 0.45$ cm w.e. $d^{-1}\,°C^{-1}$; c) scenario 2 (TWE_{max}), $\alpha_{max\ 2} = 0.58$ cm w.e. $d^{-1}\,°C^{-1}$ (intervals between the blue bars on the time axis indicate the months when snow patch #2 melted completely; blue circles indicate the estimated $TWE_{min,max}$ values from available observations; here and hereafter, blue curves correspond to $\alpha = \text{const}$, and red curves to $\alpha = f(h)$). (For interpretation of the references to color in this figure legend, the reader is referred to the web version of this article.)

4.1.2. Snow patch #1

If we apply the same PDD factors as described above ($\alpha_{min\ 2,max\ 2}$) to min and max TWE cases for snow patch #1, the snow patch completely melts out in most ablation seasons around August (Fig. 13). This contradicts observations confirming that the snow patch did not completely melt over the last four ablation seasons. Reduction of the factor to $\alpha_{min\ 1} = 0.278$ and $\alpha_{max\ 1} = 0.315$ cm w.e. $d^{-1}\,°C^{-1}$ prevents the snow patch from melting during the four critical melting periods. Instead, with these values, it gains mass and survives until September 2014 (Fig. 13). This result is surprising and will be discussed in detail below.

Satisfying the no-melt condition over the four last ablation seasons was a necessary but not sufficient condition for our model. In contrast to the case of snow patch #2, our evaluation of TWE_{year} at the beginning of each ablation period includes non-melted snow/ice from the previous year and newly hauled snow of the current year (i.e. $TWE_{year} = \Delta_{year\ -\ 1} + A_{Ayear}$, or the cumulative mass balance). Therefore, the amount of left-over snow/ice from the preceding season ($\Delta_{year\ -\ 1}$) is a major unknown for modeling snow patch #1. From this perspective, as a second step in evaluating the skill of the model to estimate the behavior of snow patch #1 over the period 2012–2014, the predicted $\Delta_{year\ -\ 1}$ should be removed from the TWE_{year}. For the fixed value of

Table 2
Main parameters of the model. Values which are different for the two snow patches are shown in bold for clarity. By 'consistency', we mean our assessment of how well each scenario agrees with the complex web of conditions discussed in the text.

Snow patch #		#2					#1					Consistency
Scenario		α_0, cm w.e. $d^{-1}\,°C^{-1}$	h_{max}, m	h_c, m	$\frac{\alpha_0}{\alpha_m}$, –	s, –	α_0, cm w.e. $d^{-1}\,°C^{-1}$	h_{max}, m	h_c, m	$\frac{\alpha_0}{\alpha_m}$, –	s, –	
TWE_{min}	i. $\alpha = \text{const}$	**0.450**	–	–	–	–	**0.278**	–	–	–	–	Poor
	ii. $\alpha = f(t)$	0.680	**0.20**	0.05	0.85	−0.6354	0.680	**0.31**	0.05	0.85	−0.6354	Medium
	iii. $\alpha = f(t)$	0.680	0.20	**0.05**	0.85	−0.6354	0.680	0.20	**0.027**	0.85	−0.6354	Good
TWE_{max}	i. $\alpha = \text{const}$	**0.580**	–	–	–	–	**0.315**	–	–	–	–	Poor
	ii. $\alpha = f(t)$	0.900	**0.20**	0.05	0.85	−0.6354	0.900	**0.38**	0.05	0.85	−0.6354	Medium
	iii. $\alpha = f(t)$	0.900	0.20	**0.05**	0.85	−0.6354	0.900	0.20	**0.027**	0.85	−0.6354	Good

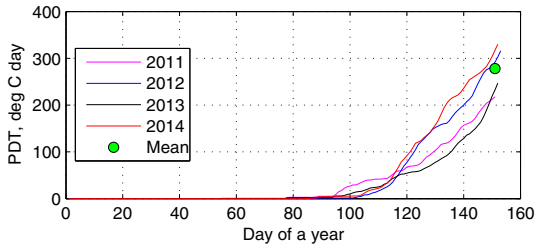

Fig. 12. Increase of positive degree day sum with time before the end of May for four spring seasons of 2011–2014.

α, such operation gives realistic results, which are close to the observed values of TWE_{year} at the beginning of the ablation season (Fig. 13). The corresponding peak melt rates in August are about 6–7 cm w.e. per day.

A difference between predicted and observed data is seen around summer 2013 and 2014 for both considered TWE scenarios (Fig. 13). Two factors could be the cause of this difference: 1) non-constant melt rates (i.e. higher in the beginning and lower towards the end of the ablation season), and 2) uncertainty in the average height during the ablation period. As already pointed out, snow patch #1 has a higher variability of surface height towards the end of each melting season than snow patch #2. For example, on 24 July 2014, the height varied between 5 and 13 m. Therefore, it is likely that the 'average height' of the ablation period may be subjective, depending on the observer, given that it is based on a visual estimation.

With our present knowledge, either explanation could be the cause of the differences between predicted and observed data. More quantitative observations will be needed to clarify this ambiguity.

4.1.3. Differences between snow patch #1 and #2

The ratio between melt rates at the first and second snow patches, α_1/α_2, indicates 38–46% less ablation at snow patch #1. However, there is no obvious explanation for such lower overall melt rates. Possible reasons include:

1) Lower ambient air temperature due to the proximity of mountains to the east of snow patch #1 (up to 1 km high; Fig. 1). Given the profile of the terrain, a major shadow effect is however unlikely. Therefore, it is unlikely that the positive air temperature (the PDD sum) would be nearly 50% lower than at snow patch #2.
2) A major insulating effect of debris cover, which as will be shown below, seems to be the most important process controlling the overall behavior of the considered systems.

At this stage, given that the first possible reason concerning lower temperatures is unlikely, the inability of the model to reproduce the behavior of both snow patches may indicate that using constant PDD factors is wrong and that debris cover changes are likely the main cause of the difference.

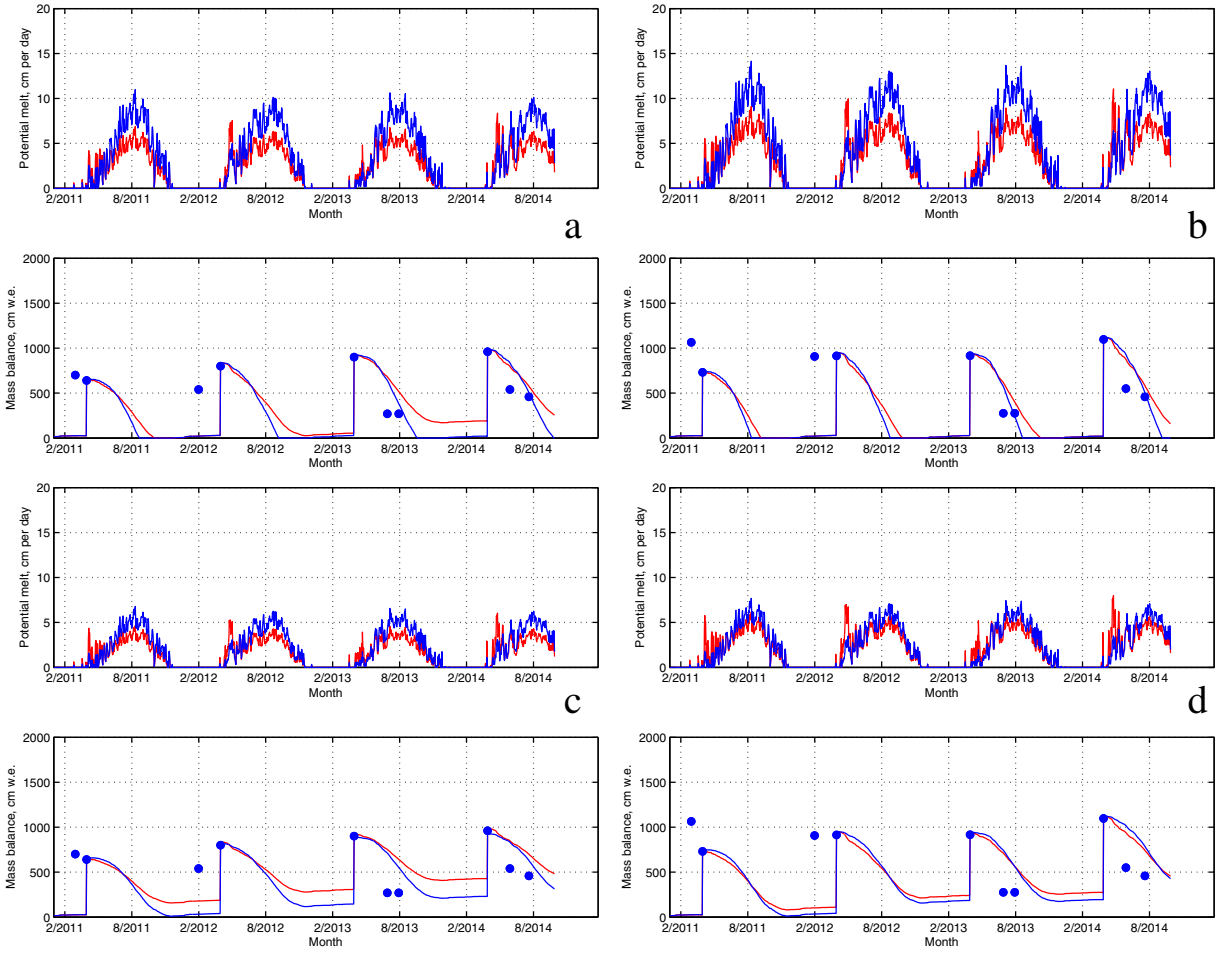

Fig. 13. Potential melting and cumulative mass-balance for 2011–2014 at snow patch #1. a) $\alpha_{min\ 2} = 0.45$ cm w.e. d^{-1} °C^{-1}; b) $\alpha_{max\ 2} = 0.58$ cm w.e. d^{-1} °C^{-1}; c) $\alpha_{min\ 1} = 0.278$ cm w.e. d^{-1} °C^{-1}; d) $\alpha_{max\ 1} = 0.315$ cm w.e. d^{-1} °C^{-1}. Blue dots indicate the estimated $TWE_{min,max}$ from available observations; blue curves correspond to $\alpha = const$, and red curves to $\alpha = f(h)$. (For interpretation of the references to color in this figure legend, the reader is referred to the web version of this article.)

4.2. Debris-modulated ablation

Owning high uncertainty and a lack of observations (see Section 3.2.2), the following may be considered only as a qualitative investigation of possible debris related effects until more measurements become available over future seasons.

The key difference between results produced by constant and non-constant PDD factor scenarios is the slightly skewed shape of the annual potential melt to the left, towards the beginning of an ablation season (Figs. 11 and 13). For particularly warm spring seasons (e.g. 2012), when debris thickness is still sub-critical, this may correspond to intensified melting with peaks reaching the same magnitude (Fig. 11) or even exceeding (Fig. 13) peaks corresponding to those produced in scenarios with constant PDD.

On the other hand, differences in mass balance temporal evolution are relatively small (Figs. 11 and 13) and cannot be used alone to validate the use of constant or non-constant PDD factor, given the limited TWE records available to us.

If we run our simulations with h_{max} for snow patch #1 higher by 11–18 cm, we obtain non-melting conditions for exactly the same α_0 and other debris-related values as for snow patch #2 (Table 2). Nevertheless, this numerical experiment is unlikely to correspond to reality, because it could not be confirmed by any observer that snow patch #1 had a nearly twice thicker debris cover than snow patch #2 (Fig. 7). Therefore, another explanation should be looked for. For example, with all parameters kept the same at both sites, a difference in h_c may be responsible for a difference in the behavior of the two snow patches. Non-melting conditions can be achieved by taking a lower $h_c = 2.7$ cm for snow patch #1 (instead of $h_c = 5$ as for snow patch #2) (Table 2). It is however unclear why this snow patch might have a lower critical thickness. One possible reason could be related to the already mentioned large amount of construction materials disposed of on this site. The lower h_c would therefore stem from the physical properties of the waste (e.g. density, permeability, and heat conductivity).

This suggests that a debris modulated behavior of the snow patches, especially of snow patch #1, is a more physically plausible explanation than air temperature differences between the sites. To check the validity of this possibility, better defined parameters of the equations of Section 3.2.2 are necessary. This could be achieved in follow-up campaigns. Furthermore, a more physical approach would be to consider the surface energy balance and a model of thermal heat transfer through the debris cover layer.

The calculated skewed annual potential melt is cascaded down the calculation line to other model outputs, such as daily discharge (Fig. 14) and surface runoff (Fig. 15).

4.3. Meltwater discharge

The total simulated amount of meltwater discharged from snow patches #1 and #2 over the period of observations is shown in Fig. 14 and was around 1×10^6 and $2–3 \times 10^6$ m^3, respectively. The overall volume is equivalent to about 1200–1600 Olympic swimming pools

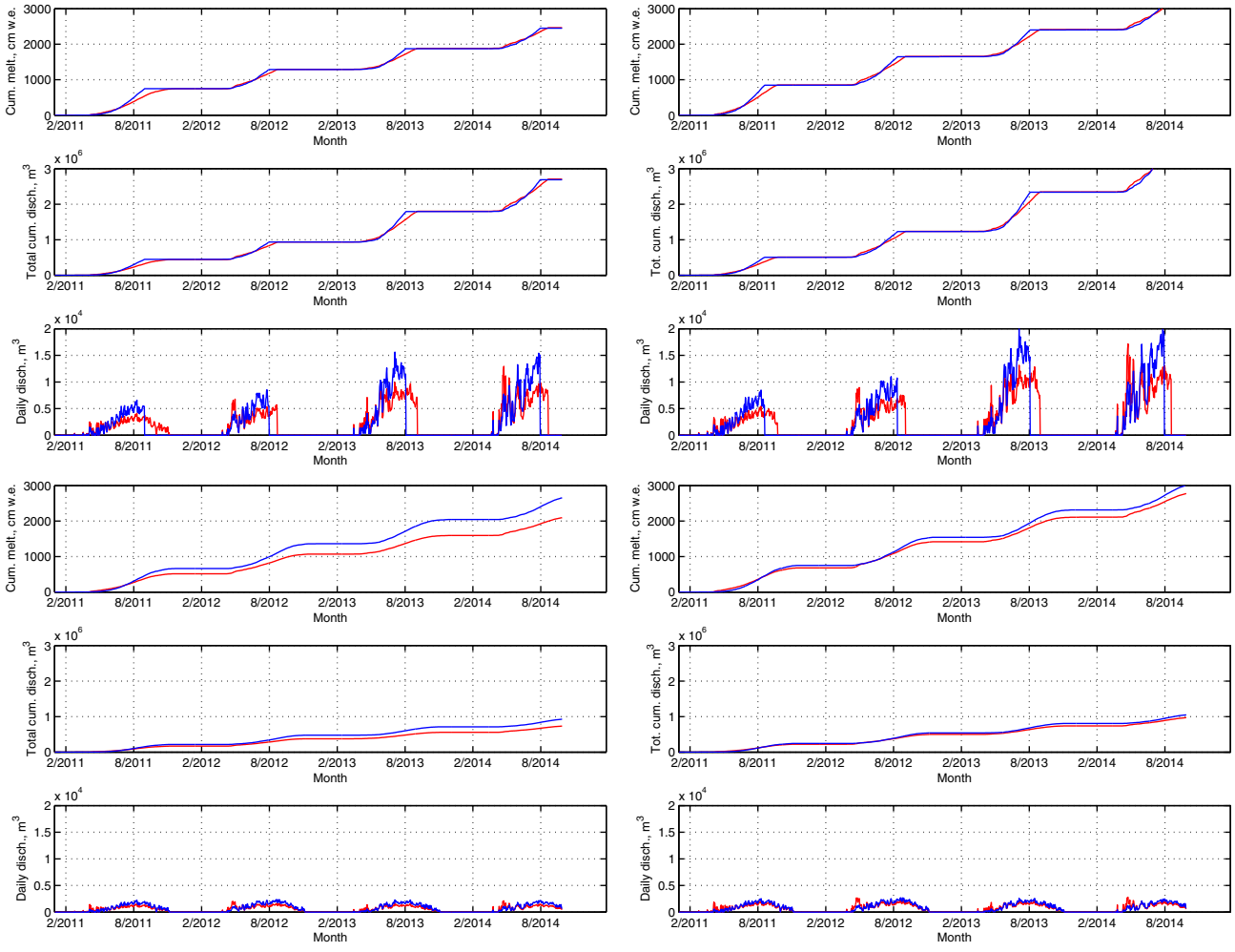

Fig. 14. Cumulative melting, total amount of meltwater discharge and daily discharge for 2011–2014 at snow patch #2 (upper 6 subpanels) and snow patch #1 (lower 6 subpanels). The left side panels are for the min TWE case; the right side panels are for the max TWE case; blue curves correspond to $\alpha = \text{const}$, and red curves to $\alpha = f(h)$. (For interpretation of the references to color in this figure legend, the reader is referred to the web version of this article.)

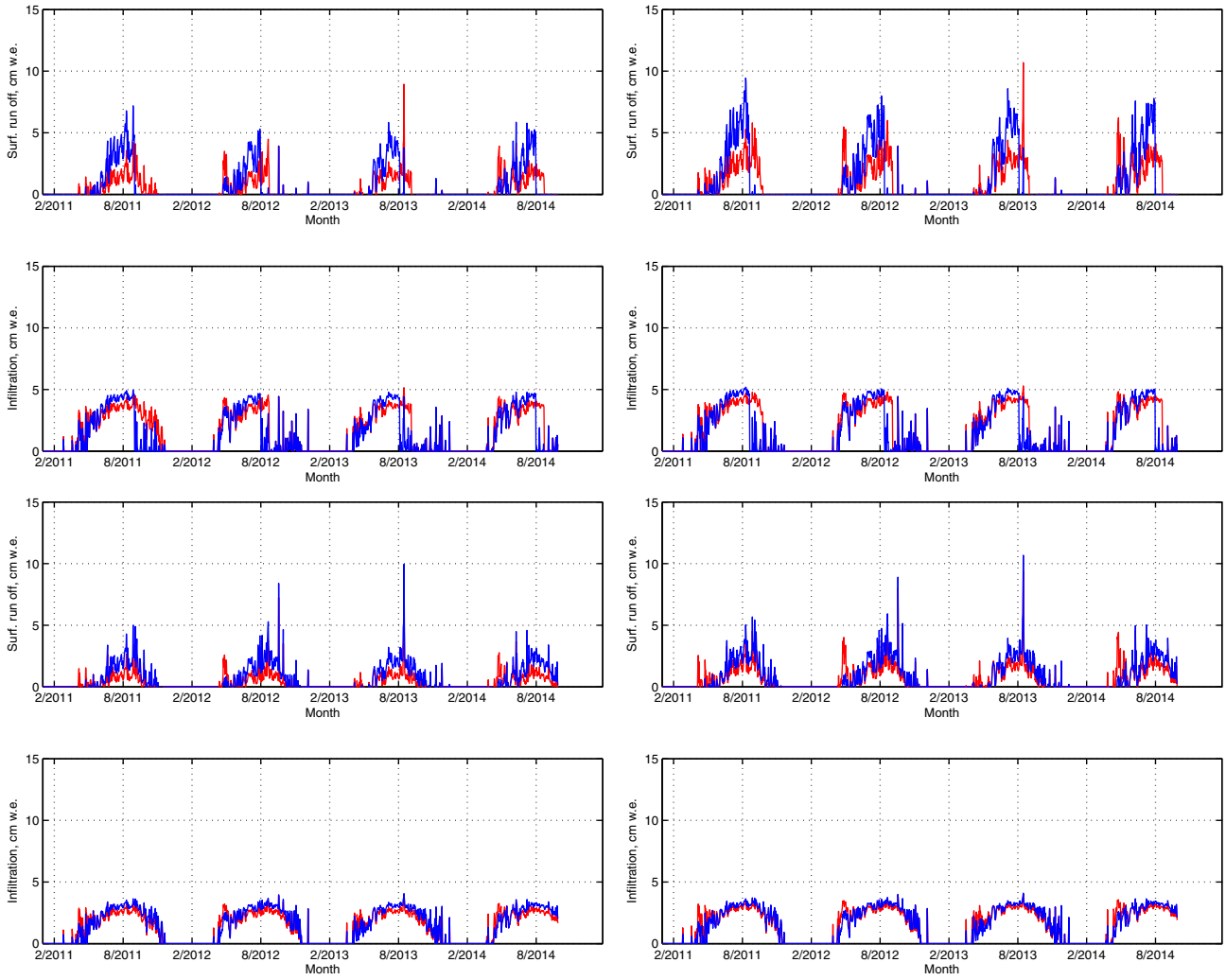

Fig. 15. Comparison between runoff/infiltration simulations made for different scenarios at both snow patches. (Snow patch #2 — upper 2 subpanels; snow patch #1 — lower 2 subpanels; left side panels — min TWE case; right side panels — max TWE case; blue curves correspond to $\alpha = \text{const}$, red to $\alpha = f(h)$). (For interpretation of the references to color in this figure legend, the reader is referred to the web version of this article.)

(a unit volume of 2500 m^3), a considerable contribution to the local urban hydrology.

Peak daily discharge is expected to occur around July–August (but can occur earlier in the event of a warm spring), with up to 15–20 $\times$ 10^3 m^3 per day from snow patch #2 and 2–4 $\times$ 10^3 m^3 per day from snow patch #1 (Fig. 14). For the same corresponding catchment area as that of the snow patches (for the beginning of melting season), typhoons may bring similar amount of water in one day (e.g. around 10 $\times$ 10^3 m^3 in August 2013 for the area of snow patch #2 or 3 $\times$ 10^3 m^3 for snow patch #1). This further illustrates the hydrological significance of these artificial snow/ice bodies, which are capable of discharging such large amounts every day for periods of weeks.

The discharge from snow patch #1 is more inter-annually homogeneous due to its relatively constant area. The discharge from snow patch #2 varies between years due to a significant change of its total area (Figs. 14 and 4).

Compared to the seasonal melting of natural snowpack (resulting river discharges peaking in May–June) (Gensiorovsky et al., 2006), artificial snow patches exhibit delayed and longer melting, which is shifted by about 3 months due to the low surface area-to-volume ratio of the patches. This also corresponds to a longer duration and local intensity of *acid flush*. The significance of this for local ecosystems remains unclear, but it may suppress vegetation due to cold acidic water input. Moreover, given that the most intense period of snow patch melting (July–August) overlaps with the period of fish spawning, the chemical influence of discharged acidic waters with pollutants may have negative effects on fish as well (e.g. Goto-Azuma, 1998).

4.4. Infiltration and surface run-off

Note that the calculated meltwater discharge may be used to evaluate infiltration and surface runoff, the latter being a melt in excess of soil infiltration (see e.g. Feiccabrino et al., 2008). Such an estimation must also consider rain rates (Fig. 6) which may affect the effective infiltration capacity.

To infer the approximate daily infiltration into soils and how much of discharge leaves as a surface runoff we used a semi-empirical Soil Conservation Service (SCS) model, a suitable approach for cases that lack data (Gabellani et al., 2008).

$$R = \frac{(P - 0.2S)^2}{P + 0.8S}, \tag{13}$$

for $P > 0.2S$, where P in our case is $= (A_B(t) + L_P(t))$, with L_P denoting rain, and

$$S = 24.5\left(\frac{1000}{CN} - 10\right), \tag{14}$$

where *CN* corresponds to a curve number parameter depending on soil type and moisture conditions (Gabellani et al., 2008). For soil conditions at snow patch #1 $CN_1 = 86$, for snow patch #2 $CN_2 = 82$.

Using this simplified approach (with results illustrated for all scenarios considered here in Fig. 15), it may be concluded that most rain leaves through infiltration, while snow patch meltwater discharge also produces a large amount of surface runoff as infiltration excess. Remarkable spikes in surface runoff from snow patch #1 in the summers of 2012 and 2013 (Fig. 15) correspond to the superimposition of meltwater discharge with rain from typhoons.

Note that the above estimates correspond to the maximum expected infiltration. In the opposite case, with negligible infiltration (i.e. $CN = 95 - 100$), almost all water from melt and rain will contribute to surface runoff (up to 15 cm w.e. per day). For example, at snow patch #2, this may be true if soil is close to saturation. This applies to snow patch #1 as well, if permafrost is present. Detailed *in situ* observations are needed to determine which conditions dominate at the sites.

Nevertheless, the inferred values of peak daily discharge and possible surface runoff provide an estimation for the required capacity of the recommended drainage/water treatment system (Lobkina and Gensiorovsky, 2012).

4.5. Chemical load

The modeled cumulative amount of presumably discharged chemical elements is shown in Fig. 16. It is directly proportional to concentrations measured in 2011 (Table 1). The largest dissolved amounts correspond to salts, which dissociate into anions and cations (Cl^-, Na^+, Ca^{2+}, Br^-). A large portion of the salts is caused by pollution, mainly involving the rock salt (NaCl) used to deice roads. Additional salt inputs are related to the seaboard geography of the regions, which affects the chemistry of precipitation due to the proximity of the sea (i.e. scavenging of marine aerosol by precipitation). Such conclusions are in line with a chemical analysis of soils at the sites, indicating salinization of soils at the base of the snow patches and in areas of snow patch meltwater discharge (Gensiorovsky et al., 2013).

The smallest cumulative amounts of discharged chemical elements are heavy metals, for example TPL_{Zn} is equal to several kg per year. Their main source is associated with vehicle exhaust accumulating in the urban snowpack.

All these estimates (Fig. 16) should be treated with caution because they are based on a single-point analysis and measurements with a greater spatial and temporal extent are required before more robust conclusions may be reached.

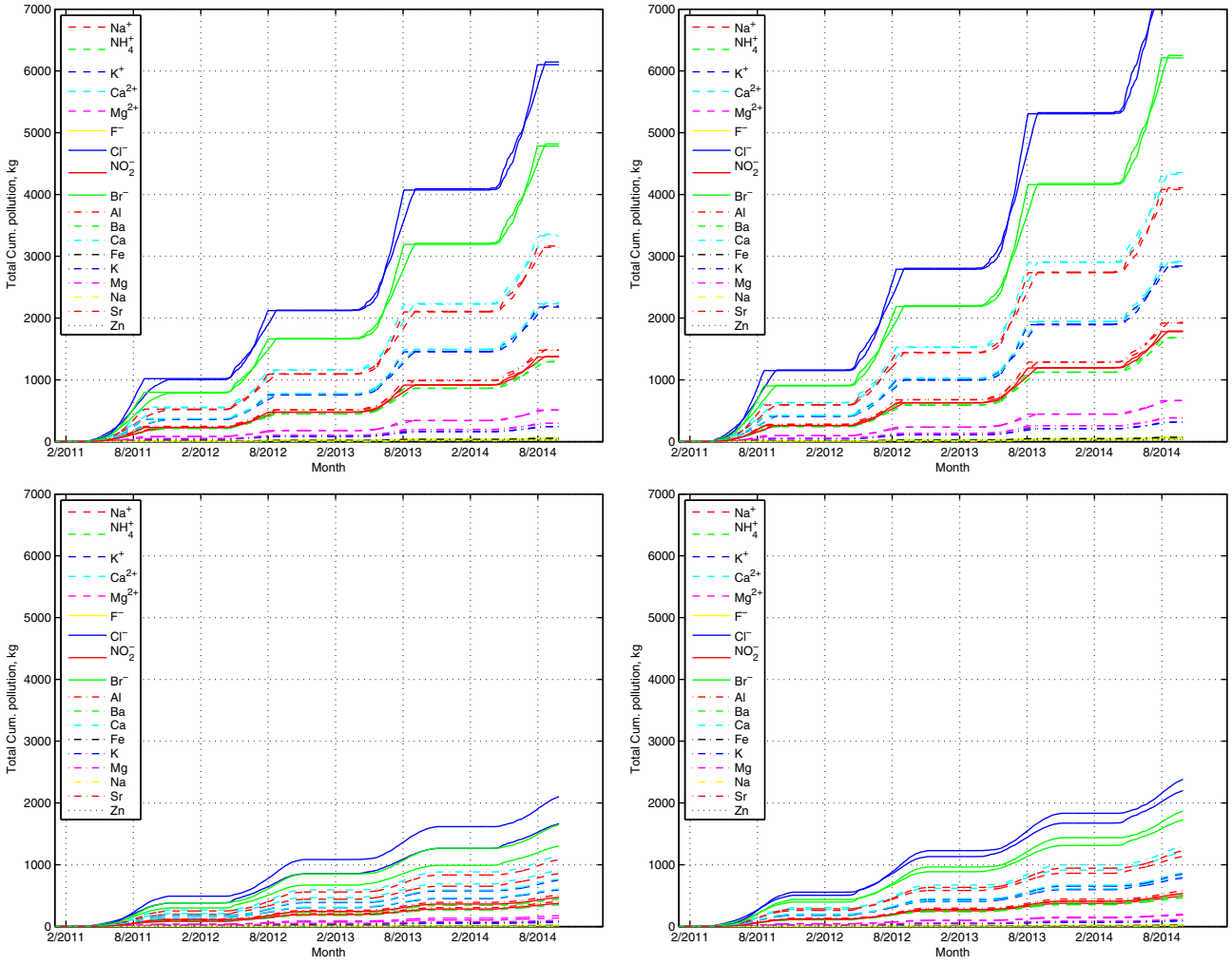

Fig. 16. Cumulative discharge of dissolved chemical elements in 2011–2014 at snow patches #2 (upper row) and #1 (lower row); the left side panels are for the min TWE case; the right side panels are for the max TWE case. Cases when α is constant or a function of debris are not shown by different colors due to small variability. (For interpretation of the references to color in this figure legend, the reader is referred to the web version of this article.)

Note also that the estimates above correspond to an average composition, which could be exceeded by an instantaneous concentration in the meltwater because of possible draining of highly concentrated liquid water inclusions between snow/ice particles or the draining of solids and particles during melting due to a fractionation process and preferential elution (Goto-Azuma, 1998).

Additionally, for example, at snow patch #2 suspended solids may contribute annually up to about $2–9 \times 10^3$ tons of material remaining after melting. Note, however, that this estimate is based on concentrations reported for another region (Feiccabrino et al., 2008) and is provided only to show an order of magnitude.

The most poorly understood process possibly taking place on the snow patches is related to photochemical ozone production/destruction during snow melt periods (Helmig et al., 2009). Another possible process is an injection of a higher solute content into the snow from the polluted supra-snow debris layer by rain. Since, to the best of our knowledge, this paper describes one of the largest anthropogenic cryospheric objects ever documented for an urban territory, it would be of interest to address such questions through future studies.

5. Summary

Optimization of snow disposal in urban areas is a difficult multi-component task, requiring consideration and analysis of many interconnected processes. To develop such a holistic procedure, we have attempted in this study to evaluate ablation and the possible environmental impact of summer melting from two artificial snow patches which are formed (or sustained) each year by snow disposal operations near the town of Yuzhno-Sakhalinsk, Russia. We employed a temperature-based melt-index model, that reasonably reproduced the overall behavior of two distinct snow/ice bodies. However, it was found that the same constant PDD factors did not make it possible to describe the evolution of the mass-balance of both snow patches. Namely, the first snow patch exhibited twice lower melt rates than the second one, despite their relatively close locations (9.7 km apart). This illustrates a peculiar case requiring investigation of a possible valley-scale environmental variability responsible for such diverging behavior despite seemingly similar environmental forcings. Furthermore, the study points out that it may be misleading to make conclusions based only on one snow patch investigated here.

After introducing a debris-modulated α factor and conducting a sensitivity analysis, we found that the same PDD factors can work well for both snow patches if debris properties differ. We suggest that the lower melt rates are associated with the quality of snow and waste disposed at the site, resulting in a debris cover that could provide a more significant insulating effect on snow patch #1.

Furthermore, we show that the timing of snow patch meltwater discharge is different from the local river hydrology driven by the melting of the natural snowpack. Snow patch meltwater could affect the local ecosystems and neighborhoods due to both the timing and the large volume of cold and polluted acidic waters they produce. Differences with previously recognized acidification of streams and lakes due to the melting of the natural snowpack (Tranter et al., 1986; Tsiouris et al., 1985) remain to be understood.

We estimate that on particularly hot days, the daily amount of meltwater discharged over the area of snow storage sites is comparable to liquid precipitation from typhoons over the same area. For the conditions of snow patch #1, a worst case scenario, an intense melting episode occurring at nearly the same time as a typhoon could produce flooding of neighboring infrastructures.

5.1. Future suggestions

It is not entirely certain that our approach to modeling melting is valid over longer periods. To complete the approach with an energy balance model, which could consider the influence of debris, and to better constrain the evolution of the described snow/ice bodies, the following set of future observations and developments is recommended to reduce random and epistemic uncertainties: 1) a regular and relatively inexpensive unmanned aerial vehicle (UAV) derived digital elevation model (DEM) to help better estimate volumetric changes over large areas of the snow patches (e.g. Ryan et al., 2014); 2) stake ablation measurements coupled with snow density profiles at several locations to reduce the uncertainty of the total water equivalent change; 3) a more spatially extensive chemical analysis of snow properties, including suspended solids, at the end of accumulation season to obtain robust chemical projections; 4) measurements of temporal and spatial variations in albedo and debris thickness to verify how exactly debris cover regulates fluctuation of snow patches through an application of more advanced energy and mass balance models such as those proposed by Bozhinskiy et al. (1986) and Nicholson and Benn (2006) or the Swiss 'SNOWPACK' model (Bartelt and Lehning, 2002; Lehning et al., 2002a, 2002b); 5) development of a physical approach to measure and model the surface energy balance and the thermal heat transfer through the debris cover layer, and 6) continuous monitoring of the water flux and water quality of nearby streams to serve as a proxy for melting and pollution discharge (Goto-Azuma, 1998).

If corroborated and documented by follow-up campaigns, the findings presented in this paper may help authorities make better informed and more sustainable decisions concerning the management of snow disposal sites. Our results already point out certain parameters that are missing and that could be very useful if measured. Finally, this case study illustrates how fundamental glaciological knowledge can provide valuable information when addressing practical geo-engineering problems.

Acknowledgments

The authors thank the Laboratory of Analytic Chemistry (FEB RAS, Far East Geological Institute, Vladivostok) for analyzing the chemical composition of snow, and H. Harder for improving the English language in the paper. We also extend our thanks to an anonymous referee and J. Schweizer for the evaluation of this manuscript and editorial work.

References

Bartelt, P., Lehning, M., 2002. A physical SNOWPACK model for the Swiss avalanche warning: part I: numerical model. Cold Reg. Sci. Technol. 35, 123–145. http://dx.doi.org/10.1016/S0165-232X(02)00074-5.

Bozhinskiy, A., Krass, M., Popovnin, V.V., 1986. Role of debris cover in the thermal physics of glaciers. J. Glaciol. 32, 255–266.

Brill, R., 1957. Structure of ice. SIPRE Tech. Rep. 33, 1–67.

Brimbelcombe, P., Clegg, S.L., Davies, T.D., Shooter, D., Tranter, M., 1987. Observation of the preferential loss of major ions from melting snow. Water Res. 21, 1279–1286.

Cadle, S., Dasch, J., Grossnickle, N., 1984. Retention and release of chemical species by a northern Michigan snowpack. Water Air Soil Pollut. 22, 303–319.

Campbell, J.F., Langevin, A., 1995a. Operations management for urban snow removal and disposal. Transp. Res. A Policy Pract. 29, 359–370. http://dx.doi.org/10.1016/0965-8564(95)00002-6.

Campbell, J.F., Langevin, A., 1995b. The snow disposal assignment problem. J. Oper. Res. Soc. 919–929.

Craigin, J., Hewitt, A., Colbeck, S., 1993. Elution of ions from melting snow: chromatographic versus metamorphic mechanisms. CRELL Rep. 93–8, 1–20.

Dominé, F., Thibert, E., 1995. Relationship between atmospheric composition and snow composition for HCl and HNO_3. In: Tonnenssen, K., Williams, M., Tranter, M. (Eds.), IAHS Publ, pp. 3–10 (chapter 228).

Dominé, F., Albert, M., Huthwelker, T., Jacobi, H.W., Kokhanovsky, A.A., Lehning, M., Picard, G., Simpson, W.R., 2008. Snow physics as relevant to snow photochemistry. Atmos. Chem. Phys. 8, 171–208. http://dx.doi.org/10.5194/acp-8-171-2008.

Feiccabrino, J., Lundberg, A., Skogsberg, K., 2008. Expected pollutant pathway differences between snow deposits and a permeable snow cooling plant. Proceedings of 65th Eastern Snow Conference (Fairlee, Vermont, USA), pp. 47–62.

Fujita, K., Hiyama, K., Iida, H., Ageta, Y., 2010. Self-regulated fluctuations in the ablation of a snow patch over four decades. Water Resour. Res. 46. http://dx.doi.org/10.1029/2009WR008383.

Gabellani, S., Silvestro, F., Rudari, R., Boni, G., 2008. General calibration methodology for a combined Horton-SCS infiltration scheme in flash flood modeling. Nat. Hazards Earth Syst. Sci. 8, 1317–1327. http://dx.doi.org/10.5194/nhess-8-1317-2008.

Gensiorovsky, Y.V., 2010. Periodicity of snowstorm winters on the Sakhalin island and problems of snowboundness of the urbanized territories. GeoRisk 4, 32–36.

Gensiorovsky, Y.V., Kazakov, N.A., 2006. Mnogoletnie snejniki o. Sakhalin: genesis i rejim [Multi-annual snow patches of Sakhalin: their genesis and regime]. Proceedings of Symposium: "Glaciologiya v kanun Mejdunarodnogo Polyarnogo Goda" ["Glaciology in the Beginning of the International Polar Year"], 9–13 October 2006, Pushkinskie Gori, Russia, p. 51.

Gensiorovsky, Y.V., Ivanova, O., Kononova, D.A., 2006. Vliyanie snejnih lavin na formirovanie stoka rek Centralnogo Sakhalina. Data Glaciol. Stud. 103, 181–183.

Gensiorovsky, Y.V., Ukhova, N., Lobkina, V., 2013. Geotechnical and ecological aspects of locating snow fields on the urbanized territory (Yuzhno-Sakhalinsk). Proceedings of International Snow Science Workshop (ISSW'13, October 7–11, 2013, Grenoble-Chamonix, France), pp. 1181–1184.

Goto-Azuma, K., 1998. Changes in snowpack and melt water chemistry during melting. In: Nakawo, M., Hayakawa, N., Goodrich, L.E. (Eds.), Snow and Ice Science in Hydrology. Institute for Hydrospheric–Atmospheric Sciences. Nagoya University and UN Educational Scientific Organization, pp. 119–133 (chapter 9).

Gross, G., 1967. Ion distribution and phase boundary potentials during the freezing of very dilute ionic solutions at uniform rates. J. Colloid Interface Sci. 25, 270–279.

Helmig, D., Cohen, L.D., Bocquet, F., Oltmans, S., Grachev, A., Neff, W., 2009. Spring and summertime diurnal surface ozone fluxes over the polar snow at Summit, Greenland. Geophys. Res. Lett. 36. http://dx.doi.org/10.1029/2008GL036549 (n/a–n/a).

Hock, R., 2003. Temperature index melt modelling in mountain areas. J. Hydrol. 282, 104–115. http://dx.doi.org/10.1016/S0022-1694(03)00257-9.

Juen, M., Mayer, C., Lambrecht, A., Han, H., Liu, S., 2014. Impact of varying debris cover thickness on ablation: a case study for Koxkar Glacier in the Tien Shan. Cryosphere 8, 377–386. http://dx.doi.org/10.5194/tc-8-377-2014.

Kayastha, R.B., Takeuchi, Y., Nakawo, M., Ageta, Y., 2000. Practical prediction of ice melting beneath various thickness of debris cover on Khumbu Glacier, Nepal, using a positive degree-day factor. Debris-covered Glaciers, Proceedings of a Workshop Held at Seattle, Washington, USA, September 2000, pp. 71–81.

Konovalov, V., 2000. Computations of melting under moraine as a part of regional modeling of glacier runoff. Debris-covered Glaciers, Proceedings of a Workshop Held at Seattle, Washington, USA, September 2000, pp. 109–118.

Lambrecht, A., Mayer, C., Hagg, W., Popovnin, V., Rezepkin, A., Lomidze, N., Svanadze, D., 2011. A comparison of glacier melt on debris-covered glaciers in the northern and southern Caucasus. Cryosphere 5, 525–538. http://dx.doi.org/10.5194/tc-5-525-2011.

Lehning, M., Bartelt, P., Brown, B., Fierz, C., 2002a. A physical SNOWPACK model for the Swiss avalanche warning: part III: meteorological forcing, thin layer formation and evaluation. Cold Reg. Sci. Technol. 35, 169–184. http://dx.doi.org/10.1016/S0165-232X(02)00072-1.

Lehning, M., Bartelt, P., Brown, B., Fierz, C., Satyawali, P., 2002b. A physical SNOWPACK model for the Swiss avalanche warning: part II. Snow microstructure. Cold Reg. Sci. Technol. 35, 147–167. http://dx.doi.org/10.1016/S0165-232X(02)00073-3.

Lobkina, V., Gensiorovsky, Y.V., 2012. Problems of placing snow polygons on urbanized territory (Yuzhno-Sakhalinsk). Vestn. DVO RAN [Trans. FEB RAS] 3, 97–102.

Lundberg, A., Feiccabrino, J., Westerlund, C., Al-Ansari, N., 2014. Urban snow deposits versus snow cooling plants in northern Sweden: a quantitative analysis of snow melt pollutant releases. Water Qual. Res. J. Can. 49, 32–42. http://dx.doi.org/10.2166/wqrjc.2013.042.

Maisincho, L., Favier, V., Wagnon, P., Basantes Serrano, R., Francou, B., Villacis, M., Rabatel, A., Mourre, L., Jomelli, V., Cáceres, B., 2014. On the interest of positive degree day models for mass balance modeling in the inner tropics. Cryosphere Discuss. 8, 2637–2684. http://dx.doi.org/10.5194/tcd-8-2637-2014.

Mayer, C., Lambrecht, A., Hagg, W., Narozhny, Y., 2011. Glacial debris cover and melt water production for glaciers in the Altay, Russia. Cryosphere Discuss. 5, 401–430. http://dx.doi.org/10.5194/tcd-5-401-2011.

Nicholson, L., Benn, D.I., 2006. Calculating ice melt beneath a debris layer using meteorological data. J. Glaciol. 52, 463–470.

Paterson, W., 1994. The Physics of Glaciers. Butterworth-Heinemann.

Reinosdotter, K., Viklander, M., 2005. A comparison of snow quality in two swedish municipalities — Lulea and Sundsvall. Water Air Soil Pollut. 167, 3–16. http://dx.doi.org/10.1007/s11270-005-8635-3.

Reznichenko, N., Davies, T., Shulmeister, J., McSaveney, M., 2010. Effects of debris on ice-surface melting rates: an experimental study. J. Glaciol. 56, 384–394. http://dx.doi.org/10.3189/002214310792447725.

Ryan, J.C., Hubbard, A.L., Todd, J., Carr, J.R., Box, J.E., Christoffersen, P., Holt, T.O., Snooke, N., 2014. Repeat UAV photogrammetry to assess calving front dynamics at a large outlet glacier draining the Greenland Ice Sheet. Cryosphere Discuss. 8, 2243–2275. http://dx.doi.org/10.5194/tcd-8-2243-2014.

Sicart, J.E., Hock, R., Six, D., 2008. Glacier melt, air temperature, and energy balance in different climates: the Bolivian Tropics, the French Alps, and northern Sweden. J. Geophys. Res. Atmos. 113. http://dx.doi.org/10.1029/2008JD010406 (n/a–n/a).

Skogsberg, K., 2005. Seasonal Snow Storage for Space and Process Cooling. (Ph.D. thesis). Lulea University of Technology, Sweden.

Skogsberg, K., Nordell, B., 2001. The Sundsvall hospital snow storage. Cold Reg. Sci. Technol. 32, 63–70. http://dx.doi.org/10.1016/S0165-232X(00)00021-5.

Suchkov, V.E., 2012. Role of Snow Drift in Redistribution of Snow Cover and Formation of Snow Patches, Glaciers and Avalanches on Sakhalin and the Kuril Islands. (Ph.D. thesis). RosHydroMet, Nalchik, Russia.

Thibert, E., Eckert, N., Vincent, C., 2013. Climatic drivers of seasonal glacier mass balances: an analysis of 6 decades at Glacier de Sarennes (French Alps). Cryosphere 7, 47–66. http://dx.doi.org/10.5194/tc-7-47-2013.

Tranter, M., Brimblecombe, P., Davies, T., Vincent, C., Abrahams, P., Blackwood, I., 1986. The composition of snowfall, snowpack and meltwater in the Scottish Highlands—evidence for preferential elution. Atmos. Environ. 20, 517–525. http://dx.doi.org/10.1016/0004-6981(86)90092-2.

Tsiouris, S., Vincent, C., Davies, T.D., Brimblecombe, P., 1985. The elution of ions through field and laboratory snowpacks. Ann. Glaciol. 7, 196–201. http://dx.doi.org/10.1016/0004-6981(86)90092-2.

Wolff, E., Mulvaney, R., Oates, K., 1989. Diffusion and location of hydrochloric acid in ice: implication for polar stratospheric clouds and ozone depletion. Geophys. Res. Lett. 19, 487–490.